BCSJ

Document type: Article

Ru/P-Containing Porous Biochar-Efficiently Catalyzed Cascade Conversion of Cellulose to Sorbitol in Water under Medium-Pressure H_2 Atmosphere

Feng Mao, Shuainan Chen, Qiao Zhang, Long Yang, Feifei Wan, Dabo Jiang, Manman Xiong, Chao Zhang, Yachun Liu, and Zaihui Fu*

National & Local Joint Engineering Laboratory for New Petro-chemical Materials and Fine Utilization of Resources, College of Chemistry and Chemical Engineering, Hunan Normal University, Changsha 410081, P. R. China

E-mail: fzhhnnu@126.com

Received: April 3, 2020; Accepted: April 27, 2020; Web Released: August 8, 2020

Zai hui Fu

Zai hui Fu, is a professor at the Institute of Fine Catalytic Synthesis, Hunan Normal University. His research interests involve molecular design of new catalytic materials, green catalytic oxidation and enzyme-like catalytic conversion. Related research achievements are published in many domestic and foreign academic journals.

Abstract

This paper discloses a simple and productive strategy for the preparation of biochar-based bifunctional catalysts. In this strategy, very cheap bamboo powder is thermally carbonized to yield P-containing porous biochars (PBCs) by the activation of concentrated phosphoric acid (H_3PO_4), and the latter can be transformed into the target catalysts *via* loading Ru nanometer particles (NPs) on them (marked as Ru/PBCs). A series of characterizations and measurements support that PBCs have stable and rich micro-meso pores and small strong acidic protons (0.10–0.28 $mmol \cdot g^{-1}$) attributable to the grafted and/or skeleton phosphorus groups, as well as a strong affinity to β-1,4-glycosidic bonds, thus exhibiting a good acid catalytic activity for the hydrolysis of cellulose to glucose. More importantly, they are excellent acidic supports for the loading of Ru NPs owing to high BET surface area, which can give the loaded Ru NPs uniform and narrow distribution (1–6 nm). The resulting bifunctional Ru/PBCs catalysts possess excellent hydrolytic hydrogenating activity for the one-pot cascade conversion of cellulose and the optimized conditions can achieve ca. 89% hexitol yield with 98% sorbitol selectivity under relatively mild conditions. This work provides a good example for the preparation of biomass-derived bifunctional catalysts and their applications in biorefinery.

Keywords: Biochars | Bifunctional catalyst | Cellulose conversion

1. Introduction

Biomass has drawn a lot of attention as an environmentally friendly and sustainable resource for the production of fuel and chemical products. Cellulosic biomass cannot be digested by humans and is very abundant in nature.[1] Therefore, cellulose is the most promising natural resource for conversion into more valuable chemicals. Cellulose can be converted into sugar alcohols, oxygenated bio-oil[2] and hydrocarbons by various chemical transformations. Especially, sorbitol, which is the hydrogenated form of glucose, is targeted in this work because it is a good model system to study the hydrolysis and then hydrogenation of cellulose. Sorbitol has been classified as one of the twelve most important bio-based platform chemicals as it can be widely used as a sweetener, a moisture controller in cosmetics, and in medical applications.[3]

Conventionally, sorbitol can be obtained by two-step conversion of cellulose, including its selective hydrolysis to glucose by acid catalysis, and then the hydrogenation of glucose by metal catalyst. A great deal of effort has been put toward the hydrolysis of cellulose to glucose with enzymes,[4] mineral acids[5] and supercritical water.[6] The obtained glucose can then be efficiently hydrogenated into sorbitol with loaded Ru nanometer particles (NPs) under relatively mild temperature (120 °C) and hydrogen atmosphere.[3] However, this two-step conversion pathway suffers from several problems such as complex operating procedures and high operating costs, relatively low conversion efficiency, as well as difficult to separate products and enzymes or mineral acids. To date, therefore, a series of investigations have been reported to direct converting

© 2020 The Chemical Society of Japan

Table 1. One-pot hydrolytic hydrogenation of cellulose using various catalysts

Catalyst	Substrate	Reaction conditions	Target product yield/%	Ref.
Ru NPs and liquid acid	cellobiose	120 °C, 12 h, 4 MPa H_2	Sorbitol (100)	7
Ru/C	cellulose	245 °C, 0.5 h, 6 MPa H_2	Hexitol (39.3)	8
H_2SO_4 and Ru/C	microcrystalline cellulose	160 °C, 5 h, 5 MPa H_2	Hexitol (60.5)	9
Pt/Al_2O_3	microcrystalline cellulose	190 °C, 24 h, 5 MPa H_2	Hexitol (31.0)	10
Ni/ZSM-5	microcrystalline cellulose	230 °C, 6 h, 4 MPa H_2	Hexitol (58.2)	11
Ni_2P/AC(1:2)	microcrystalline cellulose	225 °C, 1.5 h, 6 MPa H_2	Sorbitol (48.4)	12
Ru/$[Bmim]_3PW_{12}O_{40}$	microcrystalline cellulose	225 °C, 24 h, 6 MPa H_2	Sorbitol (44.8)	13
Ru/CNT	H_3PO_4 pre-treated cellulose	180 °C, 24 h, 5 MPa H_2	Sorbitol (69.0)	14
Ru/$NbOPO_4$-pH2	ball-milled cellulose	170 °C, 24 h, 4 MPa H_2	Sorbitol (59.6)	15
Ru/AG-CNT_{1200}	ball-milled cellulose	205 °C, 3 h, 5 MPa H_2	Sorbitol (64.1)	16
ZPA and Ru/C	ball-milled cellulose	190 °C, 2.5 h, 6 MPa H_2	Hexitol (85.5)	17
Ru-Ni/AC or Ru-Ni/CNT	ball-milled cellulose	205 °C, 1 h, 5 MPa H_2	Sorbitol (74.0 or 71.0)	18
Ru/SiO_2-SO_3H	ball-milled cellulose	150 °C, 10 h, 4 MPa H_2	Sorbitol (61.2)	19
Ru/CCD-SO_3H	ball-milled cellulose	180 °C, 10 h, 4 MPa H_2	Sorbitol (63.8)	20
Ru/AC-SO_3H	ball-milled cellulose	165 °C, 36 h, 5 MPa H_2	Sorbitol (71.1)	21
Ru/PBC	H_3PO_4 pre-treated cellulose	150 °C, 8 h, 5 MPa H_2	Sorbitol (87.1)	This Work

cellulose into sorbitol in a one-pot reaction by green and efficient ways in comparison to the above two-step conversion systems, which are summarized in Table 1. Kou et al.[7] and Liu et al,[8] successively reported two pioneering studies for this one-pot conversion reaction, the former used the PVP-stabilized Ru NP together with liquid acid as an excellent combination catalyst that could achieve the quantitative conversion of cellobiose to sorbitol, and the latter employed Ru/C and H^+ generated in situ in hot water at 245 °C to efficiently catalyze the one-pot conversion of cellulose to hexitol (39.3% yield). Subsequently, Palkovits et al.[9] reported that mineral acids together with supported metal catalysts could efficiently catalyze the one-pot conversion of cellulose to sugar alcohol, giving a 72% cellulose conversion and 84% sugar alcohol selectivity at relatively low reaction temperature and short reaction time. The extensive use of mineral acids, however, can result in difficulty in the separation of products and corrosion. Various metal NPs-loaded acidic supports, as bifunctional solid catalysts, have been developed to realize a green one-pot process to convert cellulose to sorbitol,[10–21] among them, Pt/Al_2O_3,[10] Ni/ZSM-5,[11] Ni_2P/AC(1:2)[12] and Ru/$[Bmim]_3$-$PW_{12}O_{40}$[13] can catalyze the one-pot conversion of microcrystalline cellulose in water under H_2 atmosphere, but provide low sorbitol or hexitol yield (22–58%) even using high temperature (190–230 °C) owing to the poor acidity of their supports. Ball-milled or phosphoric acid (H_3PO_4) pre-treated cellulose exhibits a high reactivity owing to the destruction of its super strong hydrogen bonding network,[14,15] and its cascade conversion catalyzed by the weak acidic bifunctional catalysts[14–18] can more efficiently proceed at relatively low temperature (170–205 °C) compared to untreated microcrystalline cellulose, affording a relatively high sorbitol or hexitol yield (64–85%). Notably, three strong acidic catalysts Ru/SiO_2-SO_3H,[19] Ru/CCD-SO_3H[20] and especially Ru/AC-SO_3H[21] exhibited a high catalysis efficiency for this one-pot cascade reaction under relatively low temperature (150–180 °C), affording 61, 64 and 71% sorbitol yields, respectively. However, these three catalysts still have some defects, including the complex or lowly efficient grafting of sulfonic groups on the supports, the high loading of Ru (10 wt%), long reaction time or unsatisfied sorbitol yield.

Recently, porous carbon materials have been investigated as potential environment-friendly adsorption materials[22] and sold acid catalysts.[23–25] Among them, the porous biochars prepared from the chemical activation of lignocellulosic materials with H_3PO_4 under moderate temperature (300–400 °C) have a stable and rich porosity as well as a small amount of strongly acidic sites through the formation of oxygen–phosphorus surface groups,[26–30] which have been successfully used to catalyze the dehydration of alcohol and conversion of starch-rich food waste into glucose and 5-HMF.[31,32] But in most instances their widespread use as robust solid acid catalysts still requires the grafting of strongly acidic sulfonic acid groups by further sulfonation with concentrated sulfuric acid.[33] Due to the above porosity and acidity, we speculate that the H_3PO_4-activated biochars (PBCs), as excellent acidic supports, may be directly used to construct robust bifunctional catalysts *via* loading metals, thereby effectively achieving the cascade conversion of cellulose to sorbitol under H_2 atmosphere in one pot. Here, we report a simple and productive strategy for the preparation of Ru-loaded PBC bifunctional catalyst. In this strategy, the P-containing porous bamboo carbon (PBC) supports can be conveniently prepared by one-step thermal carbonization of a forestry processing waste bamboo powder at moderate temperature under the activation of concentrated H_3PO_4. They can then be transformed into the desired catalysts *via* loading Ru nanometer particles (NPs) on them (marked as Ru/PBCs, see Scheme 1). A series of characterizations indicated that PBC materials have stable and rich micro-meso pores and a small amount of P-containing strong acidic groups, which are much superior to the extensively reported sulfonated biomass carbon materials obtained by two step preparation, especially in carbon skeleton stability and porosity. Moreover, PBC materials have a much stronger affinity to β-1,4-glycosidic bonds than the non-phosphate-mediated biomass carbon material, thus exhibiting a high acid catalytic activity for the hydrolysis of cellulose to glucose in water. More importantly, they, owing to high BET surface area, can bestow the loaded Ru NPs with uniform and

© 2020 The Chemical Society of Japan

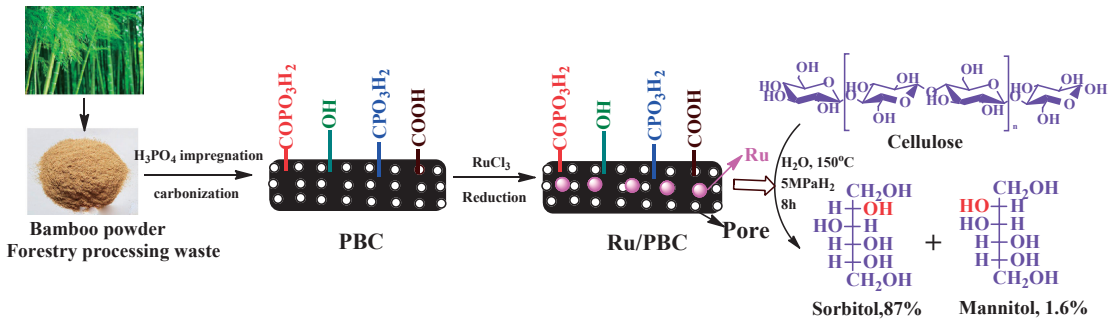

Scheme 1. Synthetic routes of Ru/PBC catalyst and its catalytic one-pot conversion of cellulose to sorbitol.

narrow distribution on them, and the resulting bifunctional Ru/PBC catalysts possess excellent hydrolytic hydrogenating activity for the one-pot cascade conversion of cellulose to sorbitol in water under medium-pressure H_2 atmosphere, which are of comprehensive advantages in catalyst availability, reaction conditions, catalysis efficiency and sorbitol yield compared to the reported hydrolytic hydrogenating catalysis systems at present.

2. Experimental Section

2.1 Reagents and Materials. Materials and reagents used in this study were forestry processing waste bamboo powder, concentrated phosphoric acid (H_3PO_4), ethylene glycol, ruthenium (III) chloride, microcrystalline cellulose (99%), cellobiose, glucose, and sorbitol, all of which were of analytical grade. Water used in the laboratory was prepared with a Millipore Milli-Q ultrapure water-purification system.

2.2 Preparation of PBC Catalyst. 10 g bamboo powder was impregnated with 85wt% H_3PO_4 (its mass ratio (X) to bamboo powder was 1, 1.5 or 2) at room temperature for 12 h, then, the impregnated samples were heated at a rate of 10 °C min^{-1} and carbonized at different temperatures (Y = 300, 350, and 400 °C) for 5 h under N_2 atmosphere, Finally, the carbonized samples were repeatedly washed with plenty of hot water and dried at 100 °C to obtain the P-containing biochars (marked as PBC-X-Y). For comparison, a direct carbonization material (marked as BC-300) of bamboo powder was also prepared at 300 °C in the absence of 85 wt% H_3PO_4.

2.3 Preparation of Ru/PBC-X-Y Catalysts. PBC-X-Y (1 g) and an appropriate amount (depending on Ru loading amount) of $RuCl_3$ aqueous solution (0.07 M) were added into a flask and stirred at room temperature for 12 h. The above mixture was evaporated at 80 °C and dried at 60 °C in a vacuum drying oven overnight. Afterwards, the dried solid was treated with 20 mL ethylene glycol at 90 °C for 8 h under magnetic stirring. Finally, the treated solid was washed repeatedly with ethyl alcohol and dried at 100 °C to obtain the desired catalysts (denoted as Z%Ru/PBC-X-Y, here, Z% indicates the theoretical loading of Ru, which was 1, 1.25, 2.5 and 5 wt%, respectively). The actual Ru loading amount of a typical sample 5%Ru/PBC-1.5-300 measured by ICP method was ca. 4 wt%.

2.4 Characterization of Catalysts. Nitrogen adsorption-desorption isotherms were measured at liquid nitrogen temperature using a Tristar 3000 fully automatic surface area and pore analyzer. X-ray photoelectron spectroscopy (XPS) of the samples was measured on a VG Multi Lab 2000 system with a monochromatic Mg-Kα source operated at 20 kV. Transmission electron microscopy (TEM) images of the samples were obtained from a JEOL JEM-2100 transmission electron microscope at an accelerating voltage of 200 kV. Transmission FT-IR spectra of the samples were recorded from 400 to 4000 cm^{-1} on a Nicolet Nexus 510P FT-IR spectroscopy using a KBr disk. Powder X-ray diffraction (XRD) analyses of the samples were conducted on a Rigaku 2550 X-ray diffractometer using Cu Kα radiation (λ = 0.15406 nm) and a graphite monochromator, operated at a voltage of 40 kV, a current of 250 mA and a slit width of 0.15 mm. XRD patterns were collected in the angular range of 10–80° with a scanning rate 2°/min. The measurement of acid density of samples by chemical titration[34–36] was performed as follows: The P-derived strong acid density was determined by ultrasonic exchange with saturated sodium chloride solution followed by titration with 0.01 mol·L^{-1} NaOH aqueous solution. The density of strong acid plus COOH and the total acid density including OH were determined by ultrasonic exchange using $NaHCO_3$ and NaOH solutions, respectively, followed by titration with 0.01 mol·L^{-1} HCl solution.

2.5 Adsorption of Cellobiose. The adsorption capacity of PBC materials on the β-1,4-glycosidic bonds was examined using cellobiose as a mimetic compound and the specific operation process of cellobiose adsorption could be found in our previous publications.[37] The obtained adsorption data indicated that PBC materials have a far stronger affinity to β-1,4-glycosidic bonds compared to BC-300 (See Supporting Information (SI), Table S1), and this unique property of PBC materials facilitates the hydrolysis of cellulose as the rate-determining step in the cascade conversion of cellulose to sorbitol.

2.6 Pre-treatment of Cellulose. Microcrystalline cellulose (15 g) was poured into 85% H_3PO_4 (150 mL) and stirred in a water bath at room temperature for 3 h and further stirred for 4 h at 50 °C. After adding a suitable amount of distilled water and stirring vigorously for 3 h, the treated solid was washed with distilled water under ultrasonic conditions until the washing water was neutral. The washed cellulose was ultrasonicated for 1 h in absolute ethanol, filtered and dried at 60 °C for 24 h to obtain the pretreated cellulose. The X-ray diffraction (XRD) pattern of microcrystalline cellulose shown in Figure S1 clearly indicated that a partial destruction of the crystal structure of cellulose occurred after treatment with 85%H_3PO_4. in agreement with previously reported results.[14]

2.7 Conversion of Cellulose to Sorbitol. 0.3 g H_3PO_4-treated cellulose, 0.1 g catalyst, and 25 mL deionized water were introduced into a 100 mL high pressure reactor, and the

© 2020 The Chemical Society of Japan

reactor was purged with 5 MPa of hydrogen gas. Then, the reaction was carried out at 150 °C with a stirring rate of 500 rpm for 8 h. After reaction, the cooled reaction samples were separated to remove the solid (a mixture of catalyst and residual cellulose) by centrifugation. After weighing the estimated residual cellulose, the recovered solid was repeatedly washed with hot water and dried at 60 °C overnight for next use as a catalyst. The obtained filtrate was analyzed with an Alltech1500 HPLC equipped with a BP-100 H^+ carbohydrate column. The eluent was diluted with H_2SO_4 solution (0.005 M) with a flow rate of 0.6 mL/min. The column and detector temperatures were 45 °C. The quantification of products was performed using an external standard method. Cellulose conversion and sorbitol yield were calculated by the following equations.

Cellulose conversion (%)
= [(added cellulose − residual cellulose)/added cellulose] × 100%

Sorbitol yield (%)
= (moles of sorbitol/moles of glucose unit in added cellulose) × 100%

3. Results and Discussion

3.1 Characterization of Catalysts. Surface Acidity: Table 2 lists the data for the yield and surface acid density of PBC-X-Y prepared by bamboo powder carbonization with different amount of H_3PO_4 at different temperatures. Entry 1 shows that the yield of BC-300 obtained by a direct carbonization of bamboo powder at 300 °C only has 34.0 wt% and its surface acidity originates from weakly acidic carboxyl (COOH, 0.21 mmol·g^{-1}) and hydroxyl (OH, 0.51 mmol·g^{-1}) groups. The use of H_3PO_4 as an activator can increase the yield of PBC-X-Y materials by 8–12 wt% and introduce 0.1–0.28 mmol·g^{-1} strong acid protons but slightly enhances the above weakly acidic groups (Entries 2–6), supporting that H_3PO_4, as supported by the P contents (0.4–4.3 wt%) measured with ICP, has been incorporated into the skeleton of PBC-X-Y materials or grafted to their surfaces in some forms, thus leading to an increase in carbonized yield and an introduction of P-containing strong acid protons.[38] Entries 3–6 further shows that enhancing the impregnated ratio of H_3PO_4 and elevating the carbonized temperature are beneficial to slightly increase the carbonization yield and the introduction of strong and weak acid groups, but the impregnated ratio shows no obvious regularity in adjusting the strong acidity. Among the prepared PBC-X-Y materials, PBC-1.5-400 has the highest strong acid content of 0.28 mmol·g^{-1}, PBC-1.5-300 has the highest total acid content of 1.48 mmol·g^{-1} and the second highest strong acid content of 0.17 mmol·g^{-1}.

Porosity: Porosity of some typical materials PBC-1.5-300 and PBC-1.5-400 as well as 5%Ru/PBC-1.5-300 and its recovered sample was measured using a low temperature nitrogen adsorption apparatus and the determined specific surface areas (S_{BET}), total pore volumes (V_p) and average porous sizes (D) are summarized in Table 3. As compared to the nonporosity of BC-300,[39] Figure 1a displays that according to the IUPAC classification, the isotherms of all the materials are of mixed type. At very low relative pressures they belong to type I with a fast-increase of N_2 uptake, which corresponds to a microporous structure.[40] At moderate and relatively high pressures, their isotherms are type IV with type H4 of broad and inconspicuous hysteresis, which can be an indicative characteristic of slit-shaped mesopores.[41] The slop of the isotherms remarkably increases with the increase of carbonization temperature, corresponding to the significant increase in S_{BET} and V_p values in Table 3. Figure 1b shows that the BJH pore distribution curves of these three materials are very narrow and similar to each other, which consist almost entirely of pores smaller than 3 nm. The porous parameters listed in Table 3 further reveal that the specific surface areas of all the materials are composed of the external ($S_{t\text{-}plot}$) and internal (S_{micro}) surface areas with different ratios and the external surface area is dominant at high carbonization temperature. Their average pore sizes are between 2.24 and 2.35 nm, and have no significant difference

Table 2. Yield of bamboo powder carbonization with H_3PO_4 under different conditions and surface acid groups of PBCs

Entry	Sample	Carbon yield /wt%	Density of acidic groups (mmol·g^{-1})			Total acidity (mmol·g^{-1})	P content[a] (wt %)
			Strong acid	-COOH	-OH		
1	BC-300	34.0	0	0.21	0.51	0.72	0
2	PBC-1-300	42.4	0.10	0.31	0.54	0.95	0.4
3	PBC-1.5-300	45.2	0.17	0.59	0.72	1.48	1.6
4	PBC-2-300	43.8	0.12	0.46	0.69	1.27	0.8
5	PBC-1.5-350	45.1	0.16	0.60	0.69	1.45	1.5
6	PBC-1.5-400	45.8	0.28	0.57	0.59	1.44	4.3

[a]Measured by ICP.

Table 3. Porous parameters of PBC-1.5-300, PBC-1.5-400 and 5% Ru/PBC-1.5-300.

Sample	S_{BET} (m^2·g^{-1})	$S_{t\text{-}plot}$ (m^2·g^{-1})	S_{micro} (m^2·g^{-1})	Pore Volume V_p (cm^3·g^{-1})	Pore Size D (nm)
PBC-1.5-300	896	419	477	0.502	2.24
PBC-1.5-400	1379	1046	233	0.811	2.35
Fresh 5%Ru/PBC-1.5-300	744	355	389	0.424	2.28
Recovered 5%Ru/PBC-1.5-300	446	189	257	0.258	2.32

© 2020 The Chemical Society of Japan

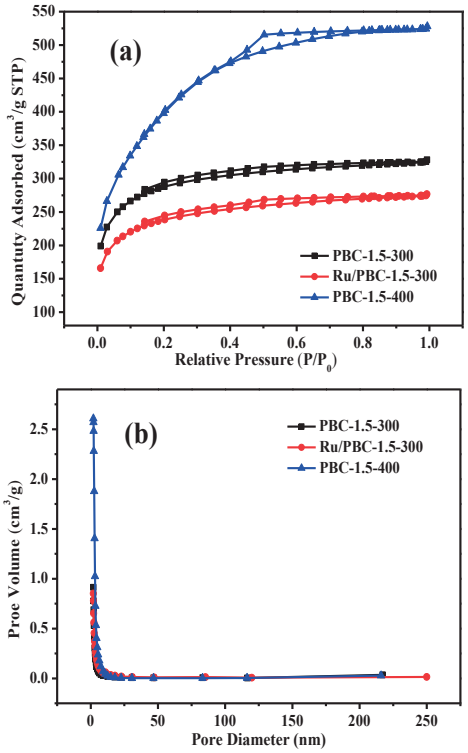

Figure 1. N_2 adsorption-desorption isotherms (a) and pore size distributions (b) for PBC-1.5-300, PBC-1.5-400 and 5%Ru/PBC-1.5-300.

between each other. Notably, the S_{BET} and V_p values of the fresh and especially recovered Ru/PBC-1.5-300 are reduced significantly compared the support PBC-1.5-300 but the D values are almost unchanged. These findings indicate that H_3PO_4 is an effective activating agent, can promote the expansion of the cellulosic structure of biomass, corresponding directly to the development of porosity. And the porosity of PBC materials is easily adjusted by varying the carbonization temperature, in consistence with the results previously reported in the literature.[29,32] The significant reduction in the porosity of 5%Ru/PBC-1.5-300 should be attributed to the micropores of the carrier occupied by the loaded Ru NPs and the further decrease in porosity after catalysis reaction may originate from the occupied effect of catalyst's micropores by the by-produced polymers in cellulose conversion.[42]

FT-IR: Figure 2 is the FTIR spectra of BC-300 and PBC-1.5-Y samples obtained using 1.5 H_3PO_4 impregnation ratio at different temperatures. In that, all the carbon materials all exhibit some characteristic absorption peaks that include stretching vibrations of OH groups in 3650–3000 cm^{-1}, COOH at 1708 cm^{-1}, Ar-OH at 1610 cm^{-1} and polycyclic aromatics in 1400–1600 cm^{-1},[43] indicating that they consist of aromatic carbon sheets with attached hydrophilic COOH and OH. Notably, two obvious IR peaks at 1200–1000 cm^{-1} can be also found in the FT-IR spectra of the P-containing materials. Among them, one peak at 1186 cm^{-1} is assigned to P=O or C-O stretching vibration in P=OOH or C-O-P groups.[44] Another peak at 1080 cm^{-1} is attributed to the symmetrical vibration of P-O-P bond in polyphosphate.[45] This indicates the existence of P-containing carbonaceous species and the incorporation of

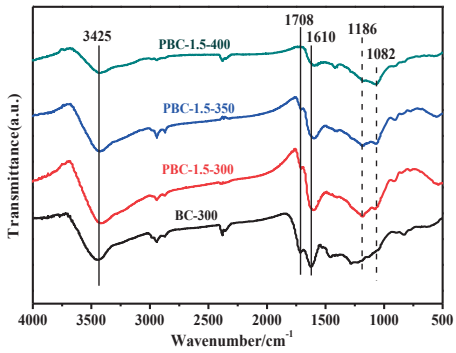

Figure 2. FTIR spectra of BC-300 and PBC-1.5-Y samples obtained using 1.5 H_3PO_4 impregnation ratio at different temperatures.

polyphosphate groups in PBC materials, as supported by ICP results in Table 2. It can be further seen from Figure 2 that as the carbonization temperature is elevated from 300 to 400 °C, the intensity of two peaks at 3425 and 1186 cm^{-1} gradually decreases, along with an increase in the peak intensity at 1080 cm^{-1}, supporting that at the high carbonization temperature, PBC material becomes hydrophobic and contains a high percentage of polyphosphate species, which the latter likely contributes to improve the incorporation of P-containing species and its derived strong acidity in PBC material, as supported by the results of Table 2.

XPS: The chemical states for the surface atoms of PBC-1.5-300 and Ru/PBC-1.5-300 were investigated by X-ray photo-electron spectroscopy (XPS) and the high resolution XPS spectra for the surface P and Ru atoms of Ru/PBC-1.5-300 are shown in Figure 3. The survey XPS spectra of these two samples and the composition of the surface elements can be found in Figure S2 and Table S2, respectively. Figure 3a shows that a broad P 2p peak with the centered binding energy of about 133.5 eV is observed in its energy spectrum, which is indicative of the characteristic of pentavalent tetracoordinated phosphorus (PO_4) as in phosphates and/or polyphosphates.[46] Further analysis by Gaussian simulation reveals the P 2p spectrum may be deconvoluted into two main characteristic peaks: One peak at 134.0 eV is assigned to phosphorus groups bound to carbon through an oxygen atom, such as C-O-PO_3H_2, (C-O)$_2PO_2H$ and (C-O)$_3PO$.[29,47,48] Another peak at 133.2 eV is C-P characteristic bonding as in C-PO_3H_2 and C_2PO_2H groups.[48] Notably, two peaks in lower binding energy that are attributed to C_3PO (132.0 eV) and C_3P (131.0 eV) groups[29] are very weak in the current P 2P spectrum, indicating that these two groups may be ignored in PBC materials. Figure 3b shows that two broad peaks for Ru $3p_{1/2}$ and Ru $3p_{3/2}$ appear centered at 483.7 and 461.4 eV, respectively, corresponding to the metallic Ru.[13,19] By further dividing above peaks gives another two weak peaks at 487.0 and 463.7 eV, which are assigned to Ru^{3+}.[13] The results support that the Ru species on Ru/PBC-1.5-300 exists mainly in metal form, and a small amount of the unreduced Ru^{3+} species is also present on the support.

XRD: As shown in Figure 4, the XRD patterns of PBC-1.5-300 and Ru/PBC-1.5-300 are very similar to each other and present two characteristic diffraction peaks at 2θ of 15–50°. The strong peak at 23.5° is assigned to amorphous carbon com-

© 2020 The Chemical Society of Japan

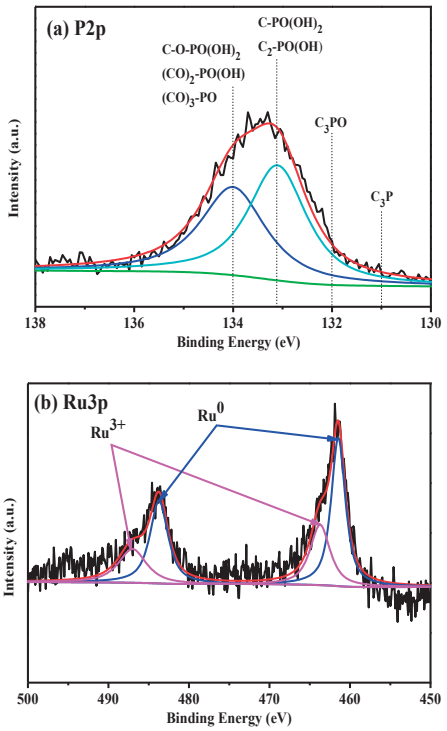

Figure 3. XPS spectra for (a) P 2p and (b) Ru 3p of 5% Ru/PBC-1.5-300.

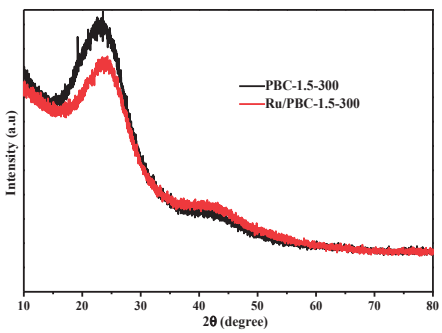

Figure 4. XRD patterns of the PBC-1.5-300 and 5%Ru/PBC-1.5-300 catalysts.

posed of aromatic carbon sheets oriented in a random fashion,[15] another weak broad peak at 35–50° is attributable to a axis of graphite structure.[49,50] Notably, a characteristic diffraction peak for meal Ru is not found in the XRD pattern of Ru/PBC-1.5-300, likely implying that the loaded Ru NPs are small size and dispersed uniformly on the support PBC-1.5-300,[15,51] as supported by the following TEM images.

TEM: Morphologies of PBC-1.5-300, 5%Ru/PBC-1.5-300 and 5%Ru/PBC-1.5-400 were observed by TEM and the obtained images are shown in Figure 5. Figure 5a shows that the dense and irregular aggregation of very small PBC NPs are clearly observed in the TEM image of PBC-1.5-300, thus rendering this carrier with a layer structure and rich slit micropores produced by PBC NPs aggregation, as supported by the $S_{t\text{-plot}}$ parameters in Table 3. A TEM image of 5%Ru/PBC-1.5-300 in Figure 5b clearly displays many black dots attributable to metal Ru NPs uniformly dispersed on PBC-1.5-300, which are attributable to metal Ru NPs, as supported by the HRTEM

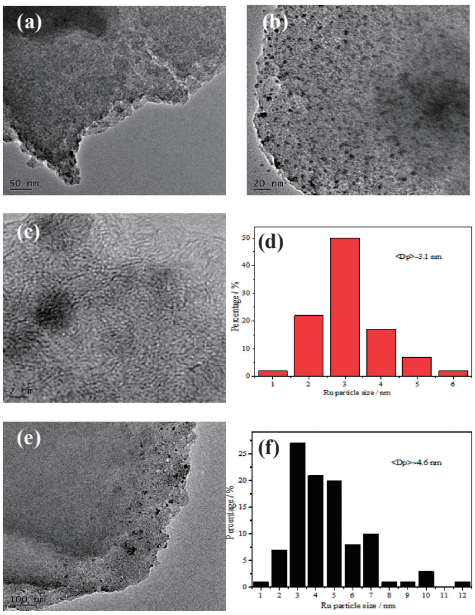

Figure 5. TEM image (a) of PBC-1.5-300, TEM image (b) and HRTEM image (c) of 5%Ru/PBC-1.5-300 and its Ru particle size distributions (d), TEM image (f) of Ru/PBC-1.5-400 and its Ru particle size distributions (e).

image in Figure 5c. The dispersed Ru NPs are all between 1 and 6 nm and their average size is ca. 3.1 nm (see Figure 5d). Unexpectedly, the dispersion of Ru NPs on the carrier PBC-1.5-400 with a higher porosity is not as good as on PBC-1.5-300 with a lower porosity (Figures 5d vs 5b), and they present a broader size distrubtion of 1–12 nm, with an average size of 4.6 nm (Figure 5e). This may be because the hydrophilicity of PBC carrier, as supported by the above FT-IR spectra, becomes worse with increasing carbonization temperature and thereby results in a decrease in the impregnation efficiency of hydrophilic precursor $RuCl_3$ into it.

3.2 Catalytic Performance of Samples for Conversion of Cellulose in Water. Table 4 lists the data for the conversion of cellulose catalyzed by various catalysts in water at 150 °C. Entry 1 shows that under hydrothermal conditions, cellulose is slightly hydrolyzed to produce a trace amount of cellobiose and glucose in the absence of catalyst. The non-phosphate activated BC-300 also exhibits a very poor activity for cellulose hydrolysis (Entry 2), which should be due to lack of strong acidity and a poor affinity to β-1,4-glycosidic bonds of cellulose, as supported by Table 2 and Table S1. In sharp contrast, all the phosphate-activated PBC-X-Y materials, due to the strong acidity and affinity to β-1,4-glycosidic bonds of cellulose, are very active for cellulose hydrolysis and can achieve 29.0–56.7% glucose and 2.1–5.5% cellobiose yields under hydrothermal conditions, along with the formation of a small amount of 5-HMF (1.2–2.7% yield, Entries 3–7). According to the difference between the above target products (32.8–62.0%) and cellulose conversion (47.7–85.3%), it is estimated that about 15–23% cellulose in this hydrolysis is converted into other by-products that may consist of soluble polymers and insoluble humins.[52] The hydrolysis activity of PBC materials increases first and then decreases with increasing the impregnation mass ratio of H_3PO_4 to bamboo powder from 1 to 2 (Entries 3–5),

© 2020 The Chemical Society of Japan

Table 4. Hydrolysis and hydrogenation of cellulose in water over various catalysts[a]

Entry	Catalyst	Conv./%	Yield of products/%				
			Cellobiose	Glucose	5-HMF	Sorbitol	Mannitol
1	No catalyst	18.6	0.3	0.5	0	0	0
2	BC-300	23.2	0.7	1.1	0.4	0	0
3	PBC-1-300	47.7	2.1	29.0	1.7	0	0
4	PBC-1.5-300	84.0 (89.5)[b]	4.2 (3.1)[b]	50.1 (54.5)[b]	1.3 (0)[b]	0 (0)[b]	0 (0)[b]
5	PBC-2-300	79.3	2.3	43.4	2.7	0	0
6	PBC-1.5-350	83.3	5.5	48.4	1.2	0	0
7	PBC-1.5-400	85.3	3.7	56.7	1.6	0	0
8[c]	PBC-1.5-300	100	0	84.1	1.7	0	0
9	Ru/PBC-1.5-300	93.7	1.8	58.6	1.0	0	0
10[b]	Ru/PBC-1.5-300	98.5	0	0	0	87.1	1.6
11[b]	Ru/PBC-1.5-350	96.8	0	0	0	80.1	1.7
12[b]	Ru/PBC-1.5-400	100	0	0	0	74.6	2.8
13[b,c]	Ru/PBC-1.5-300	100	0	0	0	90.7	1.7
14[b,d,e]	Ru/PBC-1.5-300	100	0	0	0	93.2	0.8
15[b,f]	Ru/PBC-1.5-300	37.6	0	0	0	9.2	1.0

[a]Reaction condition: cellulose, 0.3 g; catalyst, 0.1 g; H_2O, 25 mL; reaction temperature, 150 °C; reaction time, 8 h; [b]5 MPa H_2; [c]Using cellobiose as a substrate; [d]Using glucose as a substrate; [e]Reaction temperature, 120 °C; reaction time, 8 h; [f]Using microcrystalline cellulose as a substrate.

while the hydrolysis activity continuously ascends with elevating carbonization temperature from 300 to 400 °C (Entries 4, 6, 7), which well accords with the strong acidity of PBC materials in Table 2. The data in parentheses of Entry 4 shows that if this acid catalysis is performed under 5 Mpa H_2 atmosphere, glucose yield is slightly enhanced by about 4% and no 5-HMF is detected out, suggesting that under H_2 atmosphere, the efficiency of this acid catalysis hydrolysis can be improved slightly and the dehydration of glucose to 5-HMF may be also restrained. Entry 8 demonstrates that cellobiose can be completely converted to yield up to 84.1% glucose under the acid catalysis of PBC-1.5-300, revealing that it has a far higher reactivity than insoluble cellulose. Entry 9 shows that 5%Ru/PBC-1.5-300 can further improve the efficiency of cellulose hydrolysis under non-hydrogenated conditions and provide 58.6% glucose yield and a small amount of cellobiose and 5-HMF, which may stem from a contribution of its residual Ru^{3+} species as a Lewis acid.[13] Entry 10 illuminates that 5%Ru/PBC-1.5-300, as a bifunctional catalyst, can efficiently catalyze the one-step hydrolytic hydrogenation of cellulose at 150 °C under 5 Mpa H_2 atmosphere, affording up to 87.1% sorbitol yield and small amount of mannitol (1.6% yield). A comparison of two sets of data in Entries 9 and 10 may clearly find that the one-step cascade conversion of cellulose to sorbitol has a huge advantage in reducing by-products (lowering by about 13%) and enhancing the bio-derived target chemicals compared to its single-hydrolysis to glucose. This may be due to the following reasons: The loaded Ru NPs enhance the acidity of PBC carrier *via* dissociating H_2 to generate spillover H species,[53] including the above residual Ru^{3+} species. On the other hand, the Ru NPs have a good hydrogenolytic activity for the cleavage of β-1,4-glucosidic bonds of cellulose and oligosaccharides, especially an excellent activity for glucose hydrogenation,[14] thus significantly accelerating cellulose conversion into sorbitol and reducing the generation of by-products. Entries 10–12 showcase that cellulose conversion is hardly affected by the carbonization temperature of PBC carrier, but sorbitol yield presents a gradual decrease from 87.1 to 74.6% with elevating the temperature from 300 to 400 °C. This is mainly because the size and distribution of the loaded Ru NPs that are closely relative to hydrogenating activity[54] are adjusted by the carbonization temperature and the small size and uniform distribution of Ru NPs on PBC-1.5-300 carrier, as supported by the above TEM images, possess the highest hydrogenating activity. Notably, using the same catalytic conditions as Entry 10, the one-pot hydrolytic hydrogenation of cellobiose can yield up to 90.7% sorbitol yield (Entry 13), the direct hydrogenation of glucose also proceeds efficiently even at 120 °C, providing 93.2% sorbitol yield (Entry 14). But recalcitrant micro crystalline cellulose, owing to the existence of its super hydrogen bonding network,[55] has a much lower reactivity in one-pot hydrolytic hydrogenation than material treated with H_3PO_4, only providing a poor 9.2% sorbitol yield (Entry 15).

In the following experiments, we investigated the effect of variables on the one-pot hydrolytic hydrogenation of cellulose in water under 5 Mpa H_2 and the results are shown in Figures 6–9. Figure 6 gives the effect of Ru loading amount on the one-pot reaction. In that, cellulose conversion is affected by Ru loading and sorbitol yield presents a gradual increase from 76.9 to 87.1% with elevating the Ru loading from 1 to 5wt%, along with a slight increase in mannitol yield. Figure 7 displays that cellulose conversion is continuously enhanced to 100% with increasing the dosage of 5%Ru/PBC-1.5-300 catalyst and sorbitol yield first ascends and then descends when catalyst dosage is enhanced from 0.05 to 0.2 g, giving rise to a maximum of 87.1% at 0.1 g catalyst. Notably, cellobiitol, a hydrogenated product of cellobiose,[53,54] can be detected out at a low catalyst dosage of 0.05 g, while another hydrogenated product mannitol produced by fructose hydrogenation or sorbitol isomerisation[15,19] is enhanced when catalyst dosage exceeds 0.1 g. These findings support that the distribution of hydrogenated products is dominated by the strong acid amount of

© 2020 The Chemical Society of Japan

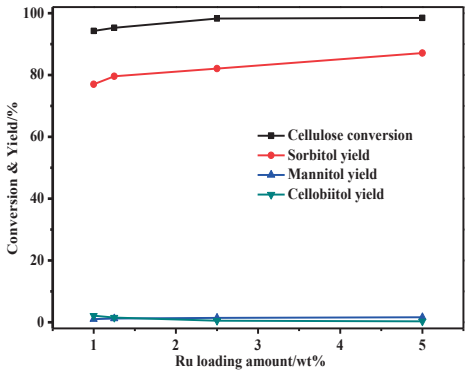

Figure 6. Effect of the Ru loading amount of catalyst on the conversion of cellulose to sorbitol. (cellulose, 0.3 g; catalyst, 0.1 g; H_2, 5 MPa; H_2O, 25 mL; reaction temperature, 150 °C; reaction time, 8 h)

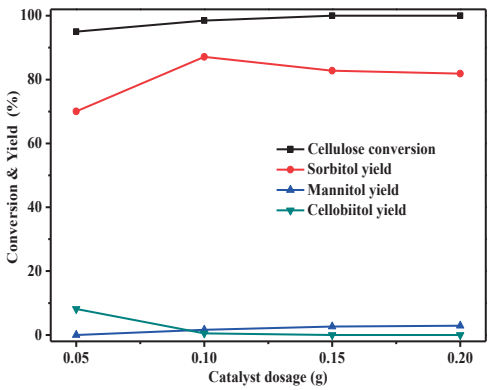

Figure 7. Effect of catalyst dosage on the conversion of cellulose to sorbitol. (cellulose, 0.3 g; H_2, 5 MPa; H_2O, 25 mL; reaction temperature, 150 °C; reaction time, 8 h.)

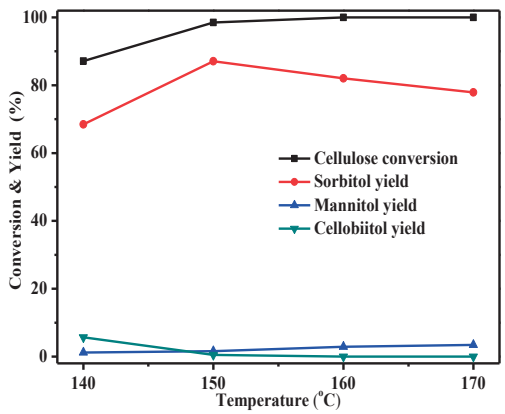

Figure 8. Effect of reaction temperature on the conversion of cellulose to sorbitol. (cellulose, 0.3 g; catalyst, 0.1 g; H_2, 5 MPa; H_2O, 25 mL; reaction time, 8 h)

catalyst determined by its dosage, the insufficient hydrolysis of cellulose to cellobiose easily occurs at low catalyst dosage, thus leading to the generation of cellobiitol. The conversion of sorbitol to mannitol and especially other unknown by-products, as supported in Table S3, can occur at high catalyst dosage, thus leading to a decrease in sorbitol. Figure 8 gives the effect of reaction temperature on the one-pot reaction catalyzed by

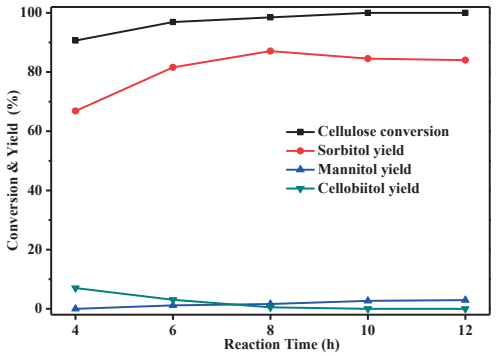

Figure 9. Effect of reaction time on the conversion of cellulose to sorbitol. (cellulose, 0.3 g; catalyst, 0.1 g; H_2, 5 MPa; H_2O, 25 mL; temperature, 150 °C)

5%Ru/PBC-1.5-300. When the reaction temperature is elevated from 140 to 160 °C, cellulose conversion is progressively enhanced from 87.1 to 100% and sorbitol yield initially rises and drops next, providing the highest 87.1% at 150 °C. The yield of mannitol slightly increases from 1.2 to 3.5% as the temperature is elevated from 140 to 170 °C. A decrease in sorbitol yield at 140 °C still originates from the insufficient hydrolysis of cellulose, which can be confirmed by an obvious increase of cellobiitol at this temperature. And its decrease at 160–170 °C likely results from higher temperature giving rise to the conversion of cellulose to undesirable by-products and fructose hydrogenation or sorbitol isomerisation to mannitol.[56] Figure 9 gives the effect of reaction time on this one-pot conversion. In that, cellulose conversion and sorbitol yield uninterruptedly rise with prolonging reaction time and respectively give rise to 98.5 and 87.1% at 8 h, along with a decrease of cellobiitol and an increase of mannitol. After that, the conversion further increases to 100% at 10 h, while sorbitol yield is slightly reduced with extending the time to 10 h, which is in agreement with stated results from the reaction temperature.

Finally, the stability of 5%Ru/PBC-1.5-300 and its carrier PBC-1.5-300 was checked by performing recycling experiments in catalytic hydrolysis and hydrogenation and the obtained results for the hydrolytic hydrogenation of cellulose in one-step and the direct hydrogenation of glucose are presented in Figure 10. As shown in Figure 10a, the hydrolytic hydrogenation efficiency of 5%Ru/PBC-1.5-300 gradually decreases with its recycling times, after three successive runs, the conversion of cellulose and the yield of sorbitol are reduced from 98.5 to 77.3% and from 87.1 to 58.8%, respectively. In sharp contrast, this catalyst exhibits an excellent reusability for the direct hydrogenation of glucose under the same reaction conditions and the hydrolytic hydrogenation efficiency hardly varies after three successive runs, still providing ca. 90% sorbitol yield (See Figure 10b). These findings indicate that the deactivation of catalyst in the hydrolytic hydrogenation of cellulose should mainly originate from leaching of its strong acid sites, as supported by the following fact: the strong acid amount of catalyst is reduced from 0.17 to 0.10 mmol·g^{-1} after three runs, corresponding to the generation and increase of cellobiitol (Figure 10a). On the other hand, a deposition of the insoluble humins formed during reaction on the acidic sites and Ru NPs of catalyst may partially contribute to catalyst deactivation. A

© 2020 The Chemical Society of Japan

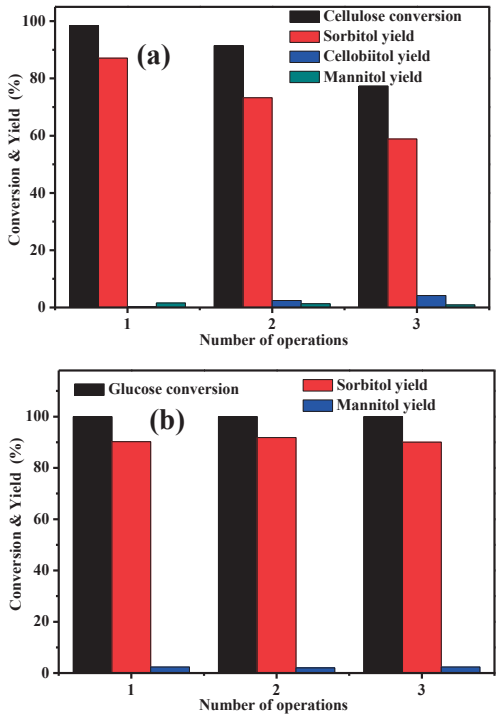

Figure 10. Recyclability of 5%Ru/PBC-1.5-300 catalyst for hydrolytic hydrogenation of cellulose (a) and direct hydrogenation of glucose (b). (Reaction condition: substrate, 0.3 g; catalyst, 0.1 g; H_2, 5 MPa; H_2O, 25 mL; reaction temperature, 150 °C; reaction time, 8 h)

direct proof to support this viewpoint is that the S_{BET} and V_p values of the recovered catalyst decline dramatically after three successive runs (See Table 3), likely owing mainly to the above deposition rather than the growth of Ru NPs or the destruction of the catalyst pore structure, as supported by the recycling result in Figure 10b. Additionally, Tables S4 and S5 give the recycling results for the hydrolysis of cellobiose and its hydrolytic hydrogenation, respectively. In that, the hydrolysis efficiency of PBC-1.5-300 and the hydrogenation efficiency of 5%Ru/PBC-1.5-300 also gradually decreases with the recycling times, but the recycling results of these two catalytic reactions are superior to that in Figure 10a. These findings indicate that the deposition of humins causing catalyst poisoning is reduced significantly, which should be due to their lower incidence in the hydrogenation of cellobiose and especially glucose compared to cellulose.

4. Conclusion

In conclusion, for the first time we have developed a simple and efficient hydrolytic hydrogenation protocol for the synthesis of sorbitol from cellulose, which has the following advantages: i) The porous PBC acidic support used in this protocol is very cheap and readily available and it can efficiently load Ru NPs to construct an excellent bifunctional Ru/PBC catalyst. ii) This protocol can efficiently achieve the one-pot cascade conversion of cellulose in a green water medium, affording ca. 89% hexitol with 98% sorbitol selectivity under relatively mild conditions (150 °C, 8 h, 5 MPa H_2). And iii) this protocol shows an excellent activity and a good reusability for the synthesis of sorbitol from the one-pot cascade conversion of cellobiose and especially the direct hydrogenation of glucose. With such kind of robust Ru/PBC catalyst in hand, we are interested in further improving the acidity and porosity of this catalyst as well as the loading efficiency of Ru NPs on it, thus significantly enhancing its hydrolytic hydrogenation performance for highly efficient synthesis of sorbitol from one-step conversion of cellulose.

We acknowledge the financial support for this work by the National Natural Science Fund of China (21676079, 21546010), the Natural Science Fund of Hunan Province (2018JJ3335, 14JJ2148, 11JJ6008, 10JJ2007), Hunan 2011 Collaborative Innovation Center of Chemical Engineering & Technology with Environmental Benignity and Effective Resource Utilization.

Supporting Information

Adsorption experiment of cellobiose, XRD patterns of Microcrystalline cellulose before and after treatment with H_3PO_4, survey XPS spectra for the PBC-1.5-300 and 5%Ru/PBC-1.5-300, further conversion of sorbitol, recyclability of PBC-1.5-300 catalyst on hydrolysis of cellobiose, recyclability of 5%Ru/PBC-1.5-300 catalyst on hydrolytic hydrogenation of cellobiose. This material is available on https://doi.org/10.1246/bcsj.20200095.

References

1 M. Jarvis, *Nature* **2003**, *426*, 611.
2 A. C. George, W. Huber, *Angew. Chem.* **2007**, *46*, 7184.
3 B. Kusserow, S. Schimpf, P. Claus, *Adv. Synth. Catal.* **2003**, *345*, 289.
4 Y. H. Zhang, L. R. Lynd, *Biotechnol. Bioeng.* **2004**, *88*, 797.
5 W. S. Mok, M. J. Antal, G. Varhegyi, *Ind. Eng. Chem. Res.* **1992**, *31*, 94.
6 M. Sasaki, Z. Fang, Y. Fukushima, T. Adschiri, K. Arai, *Ind. Eng. Chem. Res.* **2000**, *39*, 2883.
7 N. Yan, C. Zhao, C. Luo, P. J. Dyson, H. Liu, Y. Kou, *J. Am. Chem. Soc.* **2006**, *128*, 8714.
8 C. Luo, S. Wang, H. Liu, *Angew. Chem.* **2007**, *119*, 7780.
9 R. Palkovits, K. Tajvidi, J. Procelewska, R. Rinaldi, A. Ruppert, *Green Chem.* **2010**, *12*, 972.
10 A. Fukuoka, P. L. Dhepe, *Angew. Chem.* **2006**, *118*, 5285.
11 G. Liang, H. Cheng, W. Li, L. He, Y. Yu, F. Zhao, *Green Chem.* **2012**, *14*, 2146.
12 L. N. Ding, A. Q. Wang, M. Y. Zheng, T. Zhang, *ChemSusChem* **2010**, *3*, 818.
13 X. Xie, J. Han, H. Wang, X. Zhu, X. Liu, Y. Niu, Z. Song, Q. Ge, *Catal. Today* **2014**, *233*, 70.
14 W. Deng, X. Tan, W. Fang, Q. Zhang, Y. Wang, *Catal. Lett.* **2009**, *133*, 167.
15 J. Xi, Y. Zhang, Q. Xia, X. Liu, J. Ren, G. Lu, Y. Wang, *Appl. Catal., A* **2013**, *459*, 52.
16 N. R. Raap, L. S. Ribeiro, *Appl. Catal., B* **2019**, *256*, 117826.
17 Y. Liao, Q. Liu, T. Wang, J. Long, L. Ma, Q. Zhang, *Green Chem.* **2014**, *16*, 3305.
18 L. S. Ribeiro, J. J. Delgado, J. J. M. Órfão, M. F. R. Pereira, *Appl. Catal., B* **2017**, *217*, 265.
19 W. Zhu, H. Yang, J. Chen, C. Chen, L. Guo, H. Gan, X.

© 2020 The Chemical Society of Japan

Zhao, Z. Hou, *Green Chem.* **2014**, *16*, 1534.
20 Z. Li, Y. Liu, C. Liu, S. Wu, W. Wei, *Bioresour. Technol.* **2019**, *274*, 190.
21 J. W. Han, H. Lee, *Catal. Commun.* **2012**, *19*, 115.
22 P. Patnukao, P. Pavasant, *Bioresour. Technol.* **2008**, *99*, 8540.
23 S. Suganuma, K. Nakajima, M. Kitano, H. Kato, A. Tamura, H. Kondo, S. Yanagawa, S. Hayashi, M. Hara, *Microporous Mesoporous Mater.* **2011**, *143*, 443.
24 J. A. Sánchez, D. L. Hernández, J. A. Moreno, F. Mondragón, J. J. Fernández, *Appl. Catal., A* **2011**, *405*, 55.
25 L. Geng, Y. Wang, G. Yu, Y. Zhu, *Catal. Commun.* **2011**, *13*, 26.
26 J. Bedia, J. M. Rosas, J. Márquez, J. Rodríguez-Mirasol, T. Cordero, *Carbon* **2009**, *47*, 286.
27 A. M. Puziy, O. I. Poddubnaya, Y. N. Kochkin, N. V. Vlasenko, M. M. Tsyba, *Carbon* **2010**, *48*, 706.
28 J. Bedia, J. M. Rosas, D. Vera, J. Rodríguez-Mirasol, T. Cordero, *Catal. Today* **2010**, *158*, 89.
29 J. Bedia, R. Barrionuevo, J. Rodríguez-Mirasol, T. Cordero, *Appl. Catal., B* **2011**, *103*, 302.
30 M. O. G. Pérez, J. M. Rosas, R. L. Medina, M. A. Bañares, J. R. Mirasol, T. Cordero, *Catal. Commun.* **2011**, *12*, 989.
31 F. J. G. Mateos, R. Berenguer, M. J. V. Romero, J. R. Mirasol, T. Cordero, *J. Mater. Chem. A* **2018**, *6*, 1219.
32 L. Cao, I. K. M. Yu, D. C. W. Tsang, S. Zhang, Y. S. Ok, E. E. Kwon, H. Song, C. S. Poon, *Bioresour. Technol.* **2018**, *267*, 242.
33 Z. Fu, H. Wan, X. Hu, Q. Cui, G. Guan, *React. Kinet., Mech. Catal.* **2012**, *107*, 203.
34 C. Zhang, Z. Fu, Y. C. Liu, B. Dai, Y. Zou, X. Gong, Y. Wang, X. Deng, H. Wu, Q. Xu, K. R. Steven, D. Yin, *Green Chem.* **2012**, *14*, 1928.
35 C. Zhang, Z. Fu, B. Dai, S. Zen, Y. Liu, Q. Xu, S. R. Kirk, D. Yin, *Ind. Eng. Chem. Res.* **2013**, *52*, 11537.
36 C. Zhang, Z. Fu, B. Dai, S. Zen, Y. Liu, Q. Xu, S. R. Kirk, D. Yin, *Cellulose* **2014**, *21*, 1227.
37 Z. Chen, Q. Li, Y. Xiao, C. Zhang, Z. Fu, Y. Liu, X. Yi, A. Zheng, C. Li, D. Yin, *Cellulose* **2019**, *26*, 751.
38 J. Palomo, J. J. T. Hidalgo, J. M. Rosas, J. R. Mirasol, T. Cordero, *Fuel Process. Technol.* **2017**, *156*, 438.
39 J. C. P. Broekhoff, J. H. de Boer, *J. Catal.* **1967**, *9*, 8.
40 S. Brunauer, L. S. Deming, W. E. Deming, E. Teller, *J. Am. Chem. Soc.* **1940**, *62*, 1723.
41 A. M. Puziy, O. I. Poddubnaya, *Carbon* **1998**, *36*, 45.
42 J. Zhang, S. Wu, B. Li, H. Zhang, *Catal. Commun.* **2012**, *29*, 180.
43 B. Li, L. Zhou, D. Wu, H. Peng, K. Yan, Y. Zhou, Z. Liu, *ACS Nano* **2011**, *5*, 5957.
44 A. M. Puziy, O. I. Poddubnaya, A. M. Alonso, F. S. García, J. M. D. Tascón, *Carbon* **2002**, *40*, 1493.
45 S. Bourbigot, M. L. Bras, R. Delobel, P. Bréant, J. Trémillon, *Carbon* **1995**, *33*, 283.
46 A. M. Puziy, O. I. Poddubnaya, A. M. Alonso, F. S. García, J. M. D. Tascón, *Carbon* **2005**, *43*, 2857.
47 X. Wu, L. R. Radovic, *Carbon* **2006**, *44*, 141.
48 M. J. V. Romero, F. J. G. Mateos, J. R. Mirasol, T. Cordero, *Fuel Process. Technol.* **2017**, *157*, 116.
49 S. Suganuma, K. Nakajima, M. Kitano, D. Yamaguchi, H. Kato, S. Hayashi, M. Hara, *J. Am. Chem. Soc.* **2008**, *130*, 12787.
50 M. Okamura, A. Takagaki, M. Toda, J. N. Kondo, K. Domen, T. Tatsumi, M. Hara, S. Hayashi, *Chem. Mater.* **2006**, *18*, 3039.
51 B. Feng, C. Chen, H. Yang, X. Zhao, L. Hua, Y. Yu, T. Cao, Y. Shi, Z. Hou, *Adv. Synth. Catal.* **2012**, *354*, 1559.
52 D. M. Alonso, J. M. R. Gallo, M. A. Mellmer, S. G. Wettstein, J. A. Dumesic, *Catal. Sci. Technol.* **2013**, *3*, 927.
53 M. Liu, W. Deng, Q. Zhang, Y. Wang, Y. Wang, *Chem. Commun.* **2011**, *47*, 9717.
54 W. Deng, M. Liu, X. Tan, Q. Zhang, Y. Wang, *J. Catal.* **2010**, *271*, 22.
55 S. Van de Vyver, J. Geboers, P. A. Jacobs, B. F. Sels, *ChemCatChem* **2011**, *3*, 82.
56 J. Geboers, S. Van de Vyver, K. Carpentier, P. Jacobs, B. Sels, *Chem. Commun.* **2011**, *47*, 5590.

© 2020 The Chemical Society of Japan